

Neutron spin-echo spectroscopy for diffusion in crystalline solids

M. Kaisermayr,¹ M. Rennhofer,¹ G. Vogl,¹ C. Pappas,² and S. Longeville³

¹*Institut für Materialphysik d. Univ. Wien, Strudlhofg. 4, 1090 Wien, Austria*

²*Hahn-Meitner Institut, D-14109 Berlin, Germany*

³*Laboratoire Léon Brillouin, 91191 Gif-sur-Yvette Cedex, France*

(Received 18 March 2002; published 28 June 2002)

Neutron spin-echo spectroscopy (NSE) offers unprecedented opportunities in the investigation of diffusion in crystalline systems due to its outstanding energy resolution. NSE not only enables measurements at lower diffusivities than the established techniques of neutron spectroscopy, but it also gives a very immediate access to the different time scales involved in the diffusion process. This is demonstrated in detail on the example of the binary alloy NiGa where the Ni atoms hop between regular sites on the Ni sublattice and anti-sites on the Ga sublattice. Experiments on two different NSE instruments are compared to measurements using neutron backscattering spectroscopy. The potential of NSE for the investigation of jump diffusion and experimental requirements are discussed.

DOI: 10.1103/PhysRevB.66.024302

PACS number(s): 66.30.-h, 61.12.Ex

I. INTRODUCTION

Diffusion in crystals is characterized by jumps of the diffusing atoms between well defined sites where the duration of the jumps themselves is considerably shorter than the average residence times of the atoms on the lattice sites. Neutron scattering essentially contributes to the understanding of the microscopic details of diffusion in crystalline solids by providing full information on the diffusion jump, i.e., the jump frequency (or, more exactly, the residence times on different lattice sites) and the jump vector, i.e., the vector connecting the two sites between which the jump occurs.

Quasielastic neutron scattering probes the diffusive motion of atoms by means of the broadening of the elastic line (in most cases the elastic *incoherent* line) which, in a first approximation, is proportional to the jump frequencies. Due to the generally slow diffusion in crystalline solids the most powerful instruments in terms of energy resolution have to be applied in order to detect the weak quasielastic broadenings.

Up to now such experiments were performed at high-resolution backscattering spectrometers providing resolution functions with halfwidths down to approximately $1 \mu\text{ eV}$. Prominent examples are the investigation of self diffusion in sodium,¹ Li diffusion in LiC₆,² Ti diffusion in bcc-Ti,³ and diffusion of the components of intermetallic alloys.⁴ Recent experiments^{5,6} at the high resolution backscattering spectrometer IN16 of the ILL allowed one to investigate atomic motions corresponding to diffusivities around $10^{-12} \text{ m}^2/\text{s}$. With quasielastic broadenings in the range of $0.1 \mu\text{ eV}$ these measurements were definitely performed at the lower limit of what even the best backscattering spectrometer can resolve. The fact that today's world-class spectrometers have practically reached the theoretical limit (see, e.g., Ref. 7) in terms of energy resolution that can be expected from this technique, represents a severe restraint for future research in the field of diffusion in crystalline solids.

In a recent paper⁸ it was demonstrated that neutron spin-echo spectroscopy⁹ (NSE) can be applied to study diffusion in crystalline solids and that, compared to measurements

with backscattering spectrometers, significant improvements are observed. (a) Due to its high resolution NSE will allow measurements in systems with comparably slow diffusion. (b) Measurements at only two points in reciprocal space can be sufficient for an unambiguous decision between conflicting jump models. (c) NSE gives a very direct access to the different time scales involved in the diffusion process.

This paper aims at discussing in detail the experimental requirements to apply NSE to lattice diffusion and further at comparing NSE to high-resolution backscattering spectrometry. We present measurements on the two neutron spin-echo spectrometers SPAN (HMI Berlin) and MUSES (LLB Saclay) on diffusion in the well studied intermetallic model-alloy NiGa. Finally, we discuss potential future applications of NSE to diffusion in relevant intermetallic alloys.

II. THEORY

By measuring the degree of polarization of neutrons scattered on the diffusing atoms as a function of the strength of two magnetic fields, one before and one after the sample, NSE determines the coherent and incoherent intermediate scattering function $s_{\text{coh}}(\mathbf{Q}, t)$ and $s(\mathbf{Q}, t)$, i.e., the Fourier transform of the self- and pair-correlation function.⁹ With neutron resonance spin-echo spectroscopy (NRSE), the zero-field variant of NSE,¹⁰ the magnetic fields are replaced by high-frequency fields in the flippers.

A. Diffusion on non-Bravais lattices

The effect of diffusion on non-Bravais lattices on the energies of coherently scattered neutrons is not trivial because the different residence times of the atoms on the different sublattices lead to an intermediate scattering function with different relaxation times.^{11,12} According to Randl *et al.*¹³ the intermediate scattering function for diffusion between differently occupied sublattices reads:

$$s(\mathbf{Q}, t) = \sum_p^N w_p \exp(M_p t). \quad (1)$$

Hence, the quasielastic signal is a sum of N exponentials with N being the number of sublattices being “visited” by the diffusing atom. The relaxation times are given by the (negative) eigenvalues M_p of the jump matrix \mathbf{A} with matrix elements

$$A_{ij} = \frac{1}{n_{ji}\tau_{ji}} \sum_k \exp(-i\mathbf{Q}\cdot\mathbf{l}_{ij}^k) - \delta_{ij} \sum_{k'} \frac{1}{\tau_{ik'}}. \quad (2)$$

Please note that prior to diagonalization, in order to obtain real eigenvalues, \mathbf{A} has to be Hermitized by the transformation $\mathbf{B} = \mathbf{T}\mathbf{A}\mathbf{T}^{-1}$, with $\mathbf{T} = c_i^{-1/2}$. In addition the exponentials are weighted by the factors

$$w_p = \left| \sum_i \sqrt{c_i} b_i^p \right|^2 \quad (3)$$

with b_i^k denoting the i th component of the p th eigenvector of the jump matrix and c_i being the concentration of the diffusing species on the i th sublattice.

Bragg scattering can be disregarded in the present case because all measurements have been carried out sufficiently far away from reciprocal lattice points. The diffuse coherent scattering associated to the disorder in the sample is described by¹⁴

$$s_{\text{coh}}(\mathbf{Q}, t) = \sum_p w'_p \exp(M_p t) \quad (4)$$

with weights

$$w'_p = \left(\sum_i \sqrt{c_i} (\mathbf{b}^p)_i \right) \left(\sum_j (1 - c_j) \sqrt{c_j} (\mathbf{b}^{p*})_j \right). \quad (5)$$

Please note that this intensity is essentially proportional to $c_i(1 - c_i)$. Despite the high concentrations of vacancies and antistructure atoms found in NiGa (Refs. 15,16,5) this contribution can be neglected, first compared to the experimental errors of the experiments in question, and second due to the similarity of the time dependence of the diffuse coherent and incoherent contributions in the present case (for details see Ref. 14).

B. Diffusion on $B2$ lattices

$B2$ structures (or CsCl structures) are derived from bcc structures via a different occupation of the two simple cubic sublattices by two types of atoms. Diffusion of the constituents in intermetallic $B2$ alloys is mediated by the vacancy mechanism, i.e., a site exchange of an atom with a neighboring vacancy. Vacancy diffusion in these compounds can be imagined in two ways: A diffusing atom may perform a jump to a nearest-neighbor (NN) site, hence creating an antisite defect, or it may stay on its “own” sublattice by performing a jump to a next-nearest-neighbor (NNN) site. A NN jump then corresponds to a $\langle \frac{1}{2} \frac{1}{2} \frac{1}{2} \rangle$ jump while a NNN jump corresponds to a $\langle 100 \rangle$ jump.

Diffusion on a $B2$ lattice via NNN jumps is described by the Chudley-Elliot formula

$$I(\mathbf{Q}) = \exp \left[-\frac{t}{\tau} \left(1 - \frac{\Sigma}{n} \right) \right] \quad \text{with } \Sigma = \sum_k \exp(-i\mathbf{Q}\cdot\mathbf{l}_k). \quad (6)$$

Diffusion on a $B2$ lattice via NN jumps is described by Eqs. (1)–(3). The jump matrix \mathbf{A} simplifies to a (2×2) matrix with components

$$A_{11} = -\frac{1}{\tau_{\text{Ni}}}, \quad A_{12} = \frac{\Sigma}{n \tau_{\text{Ga}}}, \quad A_{21} = \frac{\Sigma}{n \tau_{\text{Ni}}}, \quad A_{22} = -\frac{1}{\tau_{\text{Ga}}}. \quad (7)$$

τ_{Ni} and τ_{Ga} denote the average residence time of a Ni atom on a site of the Ni and the Ga sublattices, respectively.

If one desires to decide between a model based on jumps on a Bravais lattice, on the one hand, and jumps between different sublattices, on the other, it is in general sufficient to perform one measurement in reciprocal space near a superlattice Bragg reflection and a second measurement near a Brillouin zone boundary. For the measurements near the superlattice point one then expects the intermediate scattering function to be nearly constant in time for jumps on a Bravais lattice, whereas a sharp decrease of the intermediate scattering function is expected for diffusion between sublattices with different local symmetry. This can be verified by substituting the corresponding scattering vector together with the jump vectors in the jump matrix, Eq. (2). On the contrary, the spectrum near the Brillouin-zone boundary depends less on the specific jump model than on the diffusion constant, hence this measurement serves as a reference. In a somewhat simplifying picture the reason for the pronounced difference of the intermediate scattering functions obtained near superlattice points for different jump models is that for jumps on a Bravais lattice a phase shift equal to zero is expected in superlattice reflections because the *jump lattice* constitutes a Bravais lattice, whereas jumps between different lattice sites produce a maximum phase shift. Hence, two measurements allow to decide between next-nearest-neighbor jumps (Bravais) and nearest-neighbor jumps (non-Bravais) in $B2$ systems. This attenuates the drawback of NSE spectrometers with respect to BS spectrometers that, up to now, NSE spectrometers cannot measure many different points in reciprocal space simultaneously. If one desires to determine the correlation factor (see following sections) a third measurement at low Q in the regime of long range diffusion has to be performed.

III. EXPERIMENT

A. Experimental requirements

The investigation of diffusion in crystalline structures demands particular qualities from spin-echo spectrometers because of the simultaneous need for high resolution and high momentum transfers. The spectrometer should allow one to access Q values of at least 1.5 to 2.0 \AA^{-1} and, at the same time, provide a dynamical range up to several nanoseconds. These two conditions are not fulfilled by most of the currently available spin-echo spectrometers because they do not

reach large scattering angles and because the energy resolution decreases significantly with decreasing wavelength.

For the experiments described here we have chosen two NSE spectrometers which fulfil the requirements mentioned above. The NSE-instruments SPAN (Berlin Neutron Scattering Center, BENSC, HMI Berlin) and MUSES (Laboratoire Léon Brillouin, CEA Saclay), allow measurements in a dynamical range up to 2–3 ns at a Q range around 1.8 \AA^{-1} , if a wavelength of about 6 \AA is chosen.

Incoherent neutron scattering is ideal for observing the diffusive motion of Ni atoms in NiGa. Four out of the five natural Ni isotopes have vanishing spin-incoherent cross sections, among them ^{58}Ni and ^{60}Ni which account for 68 and 26 % of the total isotopic composition. This leads to a practically exclusively isotope-incoherent scattering by Ni without any spin-incoherent contribution, which would spoil the beam polarization. Gallium, on the other hand, has a negligible incoherent scattering cross section, and the incoherent scattering from the Ni atoms is not disturbed by scattering from gallium atoms.

In order to obtain the temperatures needed for diffusion studies in intermetallic alloys (1000–2000 K) one uses generally Al/Nb furnaces. Both elements Al and Nb, are ideal for incoherent scattering studies, due to their low absorption and incoherent scattering cross sections. A reliable solution is the so-called “ILL-type” high-temperature furnace, which is available, e.g., at the ILL, LLB, and BENSC. In the original design the heating element of this furnace is made up of two coaxial cylinders with a diameter of 5 and 6 cm and a length of about 30 cm, thus providing a large zone of homogeneous temperature. High currents are necessary to heat the 100μ niobium sheets (e.g., $I=90\text{A}$ to obtain a temperature of $1100 \text{ }^\circ\text{C}$). These currents, however, produce strong magnetic fields which depolarize the neutron beam. Thus, a depolarization of 50% has been observed at $700 \text{ }^\circ\text{C}$ at MUSES and a depolarization of about 70% at $1100 \text{ }^\circ\text{C}$ at SPAN. Since the fields of the two cylinders cancel each other on the outside and vanish on the inside, the undesired effect is limited to the region between the two cylinders.

A considerably improved situation was achieved by a new construction comprising three cylinders. (The idea for this design was communicated to us by Petry.) In this version the cylinder in the middle conducts the current to the bottom of the heating element, while the inner and the outer cylinder lead the current back to the top. The integral over the absolute values of the magnetic field transversed by the neutrons is equal to that in the conventional construction. Now, however, the field consists of two fields with opposite orientation. Hence, the harmful effect on the neutron polarization is attenuated by the exactly opposite orientations of the field before and after the middle niobium sheet. This is due to the fact that the neutrons in the second field precess around exactly the same angle as they did in the first field, but in the reverse direction. For the present experiment a thickness of 100μ for the Nb cylinder in the middle and 50μ for the inner and outer cylinder was chosen. A smaller thickness would of course be desirable in order to reduce the necessary heating current, however, this would lead to mechanical instability.

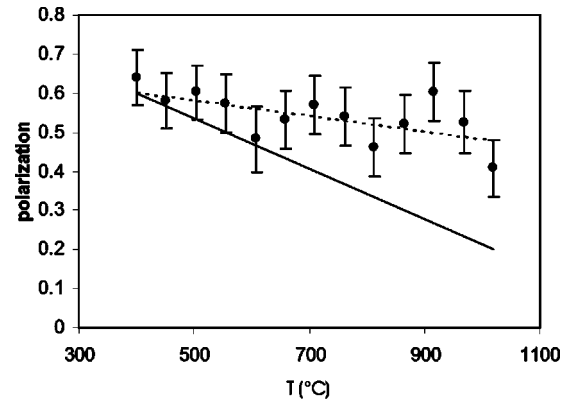


FIG. 1. Beam polarization behind the furnace as a function of the sample temperature as measured on MUSES. Solid line: Estimated evolution of the beam polarization using a conventional heating element.

Tests on these heating elements that were performed on MUSES at the LLB (Fig. 1) showed a very moderate decrease of the neutron polarization of 20% at maximum when heating up to $1100 \text{ }^\circ\text{C}$ (compare to 70% using the conventional device). This is a significant progress leading to a remarkably improved quality of the measurement. Without doubt the development of nonmagnetic heating devices will be crucial in order to benefit fully from the exceptional features that NSE provides for diffusion studies in metals.

B. Sample characteristics

For the NSE experiments we used NiGa single crystals, with near-stoichiometric compositions, i.e., a Ni content of 51.5 and 52.5 % for the measurement at SPAN and 51.5% for the measurement at MUSES. The single crystals were grown with the Chrochalski method, oriented using x-ray Laue diffractometry and cut into slices with a diameter of about 2 cm using a wire saw. The total volume of the slices was chosen such that multiple scattering rests well below 10% of the total scattering.

C. Experiment at SPAN

The spin-echo spectrometer SPAN at BENSC disposes of an unique design allowing *simultaneous* measurements at different angles.¹⁷ The neutrons precess between two flat solenoids with vertical axes and inverse current, which leads to a homogeneous radial field in the horizontal scattering plane. For a wavelength of 6.5 \AA this instrument allows one to obtain Fourier-times up to 2.5 ns, i.e., to probe sample dynamics up to 2.5 ns. With a maximum scattering angle of 135° , Q transfers up to 1.9 \AA^{-1} can be reached. For the present experiment, two detector banks covering an angle of about 10° degrees were available. The measurements at SPAN have been carried out at a wavelength of 6.5 \AA and a beam monochromatization of 16%. The detectors belonging to each of the detector banks have been grouped so that simultaneous measurements could be performed at two different angular ranges 90° – 98° (referred to as 94° in the following) and 125° – 135° (referred to as 130°), hence giv-

TABLE I. Overview over the measurements at SPAN, MUSES and IN16

$T(^{\circ}\text{C})$	at. % Ni	instrument	$D(10^{-12} \text{ m}^2/\text{s})$	$\tau_{\text{Ga}}/\tau_{\text{Ni}}$
990	51.2	IN16	1.1	
1000	51.5	MUSES	1.2	0.06(2)
1060	52.5	IN16	2.3	0.08(4)
1100	51.5	MUSES	3.7	0.12(2)
1100	51.5	SPAN	3.0	0.14(4)
1100	52.5	SPAN	3.5	0.14(4)
1130	52.5	SPAN	4.4	0.18(6)
1130	51.2	IN16	5.1	0.12(3)

ing access to a momentum transfer of 1.45 and 1.82 \AA^{-1} . Typical counting times ranged between 36 and 48 h. For the exact orientation of the single crystals please refer to Ref. 8.

The resolution function was measured two times. First, on the sample itself at 900 $^{\circ}\text{C}$, a temperature where no diffusion relevant to this type of experiment occurs in NiGa.¹⁸ Second, on a nickel disk with exactly the same geometry as the sample. This resolution measurement was carried out at 1100 $^{\circ}\text{C}$, i.e., at a temperature comparable to those applied in the experiment on NiGa, but still well below the onset of relevant diffusion in pure nickel. Both resolution functions were found to be identical within the error bars and were summed up.

D. Experiment at MUSES

The spectrometer MUSES at the LLB can be operated in two modes.¹⁹ In the *classical* option the neutrons precess along two long solenoids (longitudinal field). Each of them is replaced by two rf coils in the neutron resonance spin-echo¹⁰ (NRSE) version of the instrument. For a wavelength of 5 \AA maximum Fourier times up to 3 ns can be obtained in the NRSE mode. In the described experiment the transition from the classical mode to the NRSE mode was performed at a Fourier time of 126 ps. The scattering angle was chosen close to 100 $^{\circ}$ so that a momentum transfer corresponding to 1.85 \AA^{-1} was achieved at a wavelength of 5 \AA and a monochromatization of 15%. Counting times were around 30 h per spectrum. A NiGa single crystal with a Ni content of 51.5% was oriented such that the scattering vector was parallel to the $\langle 100 \rangle$ crystal axes. Hence the intermediate scattering function was probed at the (1.85,0,0) \AA^{-1} vector in reciprocal space which is close to the $\langle 100 \rangle$ reciprocal superlattice point of NiGa.

The measurements at MUSES have been performed using the improved amagnetic heating element described in one of the preceding sections. The resolution function was obtained from scattering on quartz at room temperature.

IV. RESULTS

A. Results from NSE experiments

The main results from the NSE experiments are summarized in Table I. In the following we will concentrate on

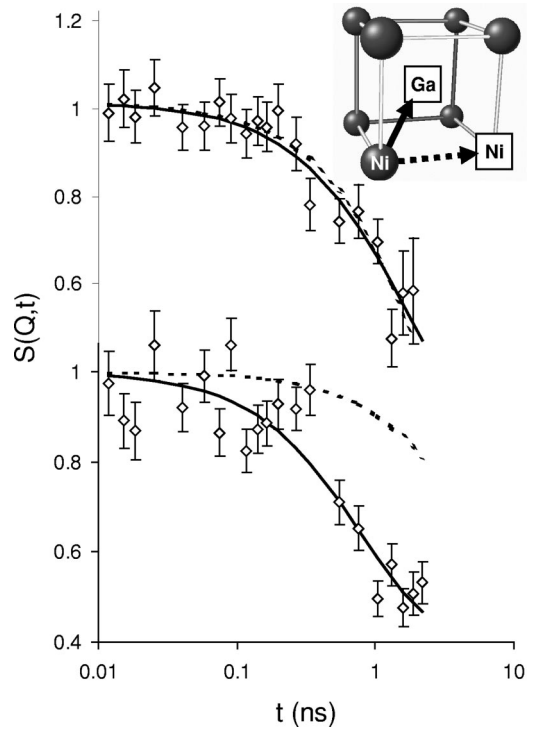


FIG. 2. Intermediate scattering function measured at SPAN on a $\text{Ni}_{52.5}\text{Ga}_{47.5}$ single crystal at a temperature of 1130 $^{\circ}\text{C}$ and at $Q = 1.45 \text{ \AA}^{-1}$ (top) and $Q = 1.82 \text{ \AA}^{-1}$ (bottom). The lines represent the intermediate scattering functions according to diffusion via nearest-neighbor jumps (solid line) and next-nearest-neighbor jumps (dashed line). Inset: Unit cell of the B2 structure. The arrows represent jumps to nearest neighbor sites (solid arrow) and next-nearest-neighbor sites (dashed arrow), respectively. This figure is taken from Ref. 8.

aspects which show the specific advantages of NSE.

Figure 2 shows the intermediate scattering function as measured on SPAN at two different scattering angles. One measurement ($Q = 1.45 \text{ \AA}^{-1}$) was performed well away from any reciprocal lattice point, whereas the \mathbf{Q} vector corresponding to the second measurement ($Q = 1.82 \text{ \AA}^{-1}$) comes close to the $\langle 100 \rangle$ reciprocal lattice point corresponding to a superlattice reflection. Thus, the second measurement allows to decide between the two conflicting jump models, whereas the first measurement serves as a reference in order to determine the diffusion constant. It is important to note that this procedure allows one to decide unambiguously between the two diffusion jumps with measurements at only two points in reciprocal space.

The very immediate access to the different time scales involved in the diffusion process is demonstrated by Fig. 3. The intermediate scattering function is a sum of two exponentials with relaxation times which are connected to the mean residence times of the Ni atoms on the two sublattices via Eqs. (1)–(3). In this example the relaxation times correspond to residence times of the Ni atoms of 6 n and 0.8 ns on the Ni and Ga sublattice, respectively. Please note, that the relaxation times do not only depend on the mean residence times, but also on the jump vectors and on the scattering vector.

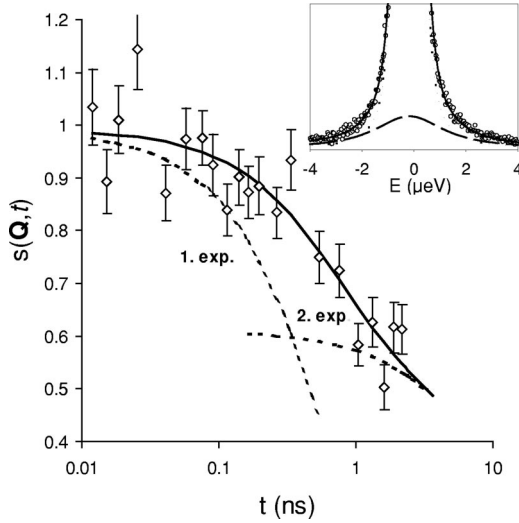


FIG. 3. Intermediate scattering function measured at SPAN on a $\text{Ni}_{52.5}\text{Ga}_{47.5}$ single crystal at 1100°C and 1.82 \AA^{-1} . The solid line, representing the intermediate scattering function as calculated on the basis of nearest-neighbor jumps, is a sum of two exponentials (dashed lines) with different relaxation times. Inset: Corresponding spectrum from a NiGa single crystal under comparable conditions (see Fig. 3 in Ref. 5). The quasielastic spectrum is a sum of two Lorentzians (dashed lines), the broad Lorentzian corresponding to the short relaxation time and the narrow Lorentzian corresponding to the long relaxation time in the main diagram.

The direct access to $s(\mathbf{Q}, t)$ mirrors in a simple and accurate determination of the ratio of residence times on the antisites and on the regular sites. The ratio $\tau_{\text{antisite}}/\tau_{\text{regular}}$, i.e., $\tau_{\text{Ga}}/\tau_{\text{Ni}}$ in the present case, gives precious information on the defect structure of the investigated alloy. With NSE this ratio can be determined from a single spectrum as is demonstrated by Fig. 4 which shows the intermediate scattering function measured on a NiGa single crystal on MUSES compared with $s(\mathbf{Q}, t)$ calculated assuming different values of this ratio.

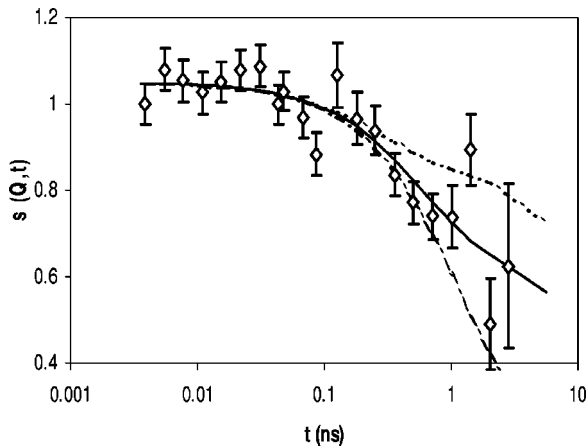


FIG. 4. Intermediate scattering function measured at MUSES on a $\text{Ni}_{51.5}\text{Ga}_{48.5}$ single crystal at 1100°C and $Q = 1.85 \text{ \AA}^{-1}$ fitted with a nearest-neighbor jump model assuming different ratios $\tau_{\text{Ga}}/\tau_{\text{Ni}}$ of the average residence times of Ni atoms on the two sublattices $\tau_{\text{Ga}}/\tau_{\text{Ni}} = 0.05$ (dotted line), $\tau_{\text{Ga}}/\tau_{\text{Ni}} = 0.12$ (solid line), $\tau_{\text{Ga}}/\tau_{\text{Ni}} = 0.3$ (dashed line).

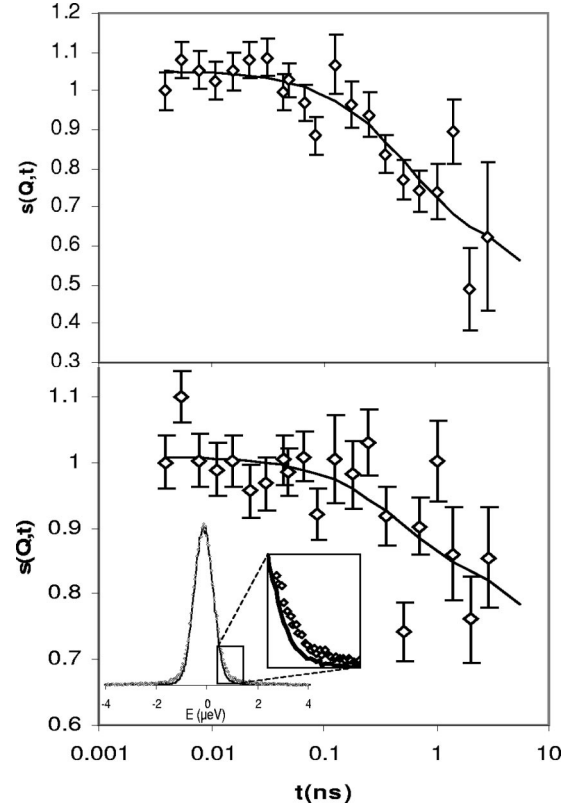


FIG. 5. Intermediate scattering function measured at MUSES on a $\text{Ni}_{51.5}\text{Ga}_{48.5}$ single crystal at 1100°C (top) and at 1000°C (bottom) with a momentum transfer corresponding to $Q = 1.85 \text{ \AA}^{-1}$. The solid line represents the intermediate scattering function according to nearest-neighbor jumps. Inset: Scattering function $S(\mathbf{Q}, \omega)$ as measured on the backscattering spectrometer IN16 on a $\text{Ni}_{51.2}\text{Ga}_{48.8}$ single crystal at 990°C (bottom) with a momentum transfer corresponding to $Q = 1.89 \text{ \AA}^{-1}$. The solid line represents the resolution function of the instrument. The region where the deviation from the resolution function becomes most important is shown enlarged.

The main interest of NSE for diffusion studies in crystalline solids is without a doubt given by its high-energy resolution. Figure 5 shows measurements on a NiGa single crystal at 1000° and 1100°C . While a 50% effect is achieved at 1100°C the maximum decrease of the intermediate scattering function amounts still to more than 20% at 1000°C , a temperature corresponding to a diffusivity of only $1.2 \times 10^{-12} \text{ m}^2/\text{s}$.

B. Comparison with data from backscattering spectrometers

The inset in Fig. 3 shows the scattering function $S(\mathbf{Q}, \omega)$ as measured at the high-resolution backscattering spectrometer IN16 at the ILL.⁵ This experiment was performed on a $\text{Ni}_{51.2}\text{Ga}_{48.8}$ single crystal at a temperature of 1130°C . Thus, the experimental conditions are comparable to those of the measurement at SPAN (shown in the main diagram of Fig. 3) where Ni diffusion in a $\text{Ni}_{52.5}\text{Ga}_{47.5}$ single crystal was measured at 1100°C . Hence, comparable diffusivities $5.1 \times 10^{-12} \text{ m}^2/\text{s}$ at IN16 and $3.0 \times 10^{-12} \text{ m}^2/\text{s}$ at SPAN, were observed. The comparison of the two spectra shows that the

access to the two time scales associated to the different average residence times on the two sublattices is much more direct for the NSE measurement. The deviation of $s(\mathbf{Q}, t)$ as determined with NSE from a *single exponential* can be recognized with the naked eye, whereas one has to trust the computer for the deviation of $S(\mathbf{Q}, \omega)$ as determined with a backscattering spectrometer from a single Lorentzian. In addition, a comparably large number of spectra, in the order of 10 to 20, has to be collected on a backscattering spectrometer in order to determine the ratio of the two residence times.

Figure 5 illustrates the remarkably high resolution of the NSE measurements. The intermediate scattering function $s(\mathbf{Q}, t)$ shown in the bottom graph was measured on MUSES on a NiGa single crystal at 1000 °C. The scattering function $S(\mathbf{Q}, \omega)$, shown in the inset, was measured at IN16 at 990 °C. Despite the comparable diffusivities, 1.1×10^{-12} and 1.2×10^{-12} m²/s, the NSE measurement shows an effect of around 20% (i.e., a decrease of the intermediate scattering function from 1.0 to approximately 0.8) whereas the quasi-elastic broadening observed with the backscattering spectrometer is extremely weak. The deviation of the broadened line from the elastic resolution function is only discernible due to the outstandingly high quality of both, the resolution function and the actual spectrum. The large quasielastic effect, even at low diffusivities, is the reason why it was possible to determine the ratio of residence times on the two sublattices at 1000 °C at SPAN while the lowest temperature where this parameter could be determined at a backscattering spectrometer was 1060 °C (Ref. 5). Taking into account that it will be difficult to improve the experimental conditions at the backscattering spectrometer, both in terms of instrumental parameters and sample environment and that, on the other hand, the experiments on the NSE spectrometers are early measurements of this kind with a high potential for future developments the sample environment and the instruments themselves, it becomes clear that NSE will allow diffusion studies at considerably lower diffusivities than does backscattering spectrometry.

The advantage of backscattering spectrometers, which measure at several points in reciprocal space simultaneously, is attenuated by the fact that two measurements with NSE spectrometers will be generally sufficient to characterize the diffusion jump. Only a third measurement, which then has to be performed at small Q , is necessary if the *correlation factor* shall be determined. The correlation factor f sets the frequencies of individual jumps in relation to long range diffusion via

$$f = D/D', \quad (8)$$

with D being the long range diffusivity and D' being the diffusivity one expects for atoms diffusing with a given jump frequency on an *empty* lattice, i.e., for a completely stochastic motion. This information on the time correlation of subsequent jumps allows one to decide between competing models of correlated atom-vacancy motion.²⁰ While jump frequencies can be obtained from neutron scattering at high Q (i.e., Q higher than 1 \AA^{-1} approximately) the long range diffusivity D can be retrieved from radio-tracer experiments

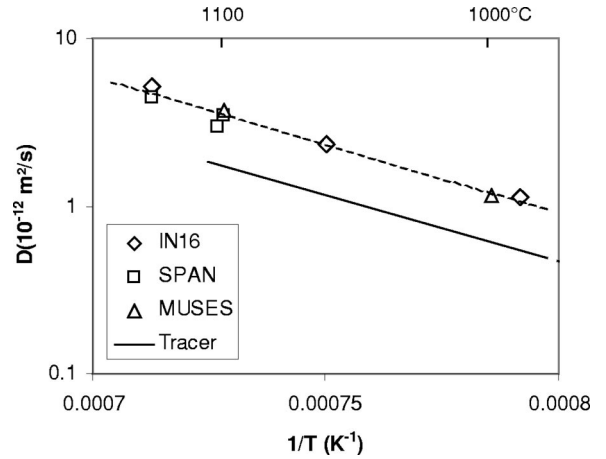


FIG. 6. Diffusivities as measured on NiGa single crystals with Ni contents between 51.2 and 52.5 % with the spin-echo spectrometers SPAN and MUSES as well as with the backscattering spectrometer IN16. The dotted line is the Arrhenius fit to the neutron data. The solid line are diffusivities from tracer diffusion measurements (Ref. 18) on Ni₅2.4Ga₄7.6. The difference between neutron and tracer data can be attributed to the correlation factor (see text).

(see, e.g., Ref. 21) or, alternatively, from QNS measurements in the hydrodynamic limit, i.e., at small momentum transfers. Of course, the latter method is the more reliable one because it allows one to measure D under *exactly* the same conditions as D' . Given the sharp dependence of diffusivities on the sample temperature this is a crucial point. Thus, NSE is expected to emerge as the ideal tool for the accurate determination of correlation factors because the high resolution provided by this method particularly at small Q compensates the decreasing quasielasticity of the signal when small momentum transfers are approached.

Figures 6 and 7 show that the diffusion parameters D and $\tau_{\text{Ga}}/\tau_{\text{Ni}}$, determined at the two NSE spectrometers and on the backscattering spectrometer agree well with each other. The comparison of the diffusivities obtained by neutron scattering with tracer data¹⁸ indicates a correlation factor of

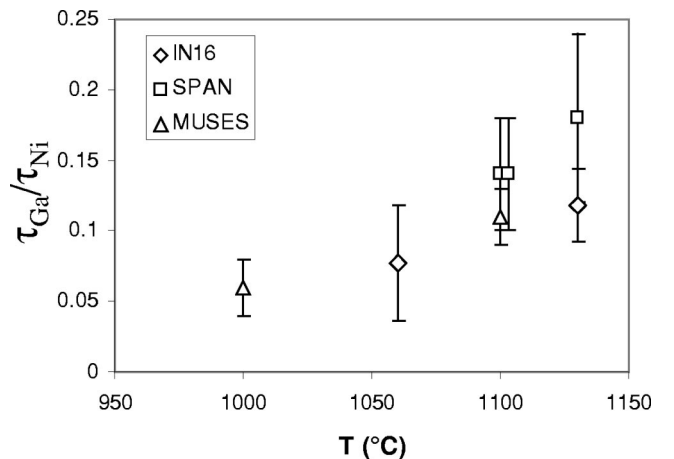


FIG. 7. Ratio of mean residence times $\tau_{\text{Ga}}/\tau_{\text{Ni}}$ of the Ni atoms on the two sublattices measured on NiGa single crystals with Ni contents between 51.2 and 52.5 %.

about 0.5 defined by Eq. (8) (see also Ref. 20). The fact that in Fig. 7 the value for $\tau_{\text{Ga}}/\tau_{\text{Ni}}$ at 1130 °C obtained at SPAN is somewhat higher than that obtained at IN16 can be attributed to the more off-stoichiometric composition of the sample used at IN16 which is connected to higher concentrations of antisite atoms and therewith longer mean residence times of the diffusing atoms on the antisites.

V. CONCLUSION

Experiments on two neutron spin-echo spectrometers of a substantially different type showed that NSE can be advantageously used for the investigation of diffusion in crystalline solids using both classical NSE and the zero-field technique NRSE. As in backscattering spectrometry, the technique conventionally used for this type of investigations, NSE provides the entire information on the microscopic diffusion mechanism: length and direction of the jump vector, jump frequencies or residence times on the different sublattices, and the correlation factor relating long range diffusion to frequencies of individual jumps.

The definite advantages of NSE are (a) the immediate access to the different time scales involved in the diffusion process and, most important, (b) the excellent energy resolution. NSE gives access to longer times than any other spectroscopic method based on neutron scattering. This is most essential for the investigation of diffusion in crystalline solids where the uncorrelated motion of atoms is in general comparably slow. NSE will therefore allow moves studies on

systems which were previously inaccessible to inelastic neutron spectroscopy. Examples are intermetallic alloys on the transition metal poor side and systems at relatively low temperatures. Particularly interesting are alloys with high ordering energies such as NiAl or the technically important super alloys, where no direct information on the diffusion process on the microscopic scale is available.

The comparison with experiments using high-resolution neutron backscattering spectrometry demonstrates two points. First, NSE is already better suited to the investigation of diffusion on crystalline solids and especially on intermetallic alloys. Second, NSE experiments have a high potential for improvements and very probably spin-echo spectroscopy will outrun backscattering techniques for diffusion studies in crystalline alloys in the near future. Immediate improvements will be achieved by the use of nonmagnetic heating devices. Future spin-echo spectrometers, that are designed for measurements at high momentum transfers, could further push the accessible dynamical range towards longer times.²²

ACKNOWLEDGMENTS

The authors are indebted to A. Triolo for assistance with one of the the experiments and to H. Schicketanz for help with the sample preparation as well as to B. Sepiol for precious advice. We also thank W. Petry for communicating to us the idea for the nonmagnetic heating device. M.K. acknowledges the financial support by BENSC and the European Commission (Contract No. HPRI-CT-1999-00020).

-
- ¹M. Ait-Salem, T. Springer, A. Heidemann, and B. Alefeld, *Philos. Mag. A* **39**, 797 (1979).
- ²A. Magerl, H. Zabel, and I. Anderson, *Phys. Rev. Lett.* **55**, 222 (1985).
- ³W. Petry, T. Flottmann, A. Heiming, J. Trampenau, M. Alba, and G. Vogl, *Phys. Rev. Lett.* **61**, 722 (1988).
- ⁴G. Vogl, M. Kaisermayr, and O.G. Randl, *J. Phys.: Condens. Matter* **8**, 4727 (1996).
- ⁵M. Kaisermayr, J. Combet, H. Ipser, H. Schicketanz, B. Sepiol, and G. Vogl, *Phys. Rev. B* **61**, 12 038 (2000).
- ⁶M. Kaisermayr, J. Combet, H. Ipser, H. Schicketanz, B. Sepiol, and G. Vogl, *Phys. Rev. B* **63**, 054303 (2001).
- ⁷R. Hempelmann, *Quasielastic Neutron Scattering and Solid State Diffusion* (Clarendon Press, Oxford, 2000).
- ⁸M. Kaisermayr, C. Pappas, B. Sepiol, and G. Vogl, *Phys. Rev. Lett.* **87**, 175901 (2001).
- ⁹F. Mezei, in *Neutron Spin Echo*, edited by F. Mezei (Springer, Berlin, 1980), p. 3.
- ¹⁰R. Gähler and R. Golub, *Z. Phys. B: Condens. Matter* **65**, 269 (1987).
- ¹¹J.M. Rowe, K. Skld, H.E. Flotow, and J.J. Rush, *J. Phys. Chem. Solids* **32**, 41 (1971).
- ¹²K.W. Kehr, D. Richter, and R.H. Swendsen, *J. Phys. F: Met. Phys.* **8**, 433 (1978).
- ¹³O.G. Randl, B. Sepiol, G. Vogl, R. Feldwisch, and K. Schroeder, *Phys. Rev. B* **49**, 8768 (1994).
- ¹⁴M. Kaisermayr, B. Sepiol, and G. Vogl, *Physica B* **301**, 115 (2001).
- ¹⁵A.H.V. Ommen, *Phys. Solid State* **72**, 273 (1982).
- ¹⁶K. Ho, M.A. Quader, F. Lin, and R.A. Dodd, *Scr. Metall.* **11**, 1159 (1977).
- ¹⁷C. Pappas, G. Kali, T. Krist, P. Boni, and F. Mezei, *Physica B* **283**, 365 (2000).
- ¹⁸A.T. Donaldson and R.D. Rawlings, *Acta Metall.* **24**, 285 (1976).
- ¹⁹M. Koeppel, P. Hank, J. Wuttke, W. Petry, R. Gähler, and R. Kahn, *J. Neutron Res.* **4**, 261 (1996).
- ²⁰M. Kaisermayr, J. Combet, B. Sepiol, and G. Vogl, *Defect Diffus. Forum* **194-199**, 461 (2001).
- ²¹H. Mehrer, *Mater. Trans., JIM* **37**, 1259 (1996).
- ²²C. P. G. Ehlers, B. Farago, and F. Meyer (unpublished).